

Isotope Effect on Anharmonic Thermal Atomic Vibration and κ Refinement of ^{12}C and ^{13}C Diamond

T. YAMANAKA^a AND S. MORIMOTO^b

^aDepartment of Earth and Space Science, Faculty of Science, Osaka University, 1–16 Machikaneyama Toyonaka, Osaka 560, Japan, and ^bDepartment of Physics, Faculty of Material Engineering Sciences, Osaka University, 1–3 Machikaneyama Toyonaka, Osaka 560, Japan

(Received 2 July 1994; accepted 1 August 1995)

Abstract

Isotope dependence of diamond structure of the mixed crystals of $^{13}\text{C}_x^{12}\text{C}_{(1-x)}$, which were grown under high pressure, has been examined by diffraction study using synchrotron radiation. The lattice constant is expressed by

$$a(\text{\AA}) = 3.56712(5) - [9.01(5) \times 10^{-4}X] + [3.65(4) \times 10^{-4}X^2],$$

where $X = [^{13}\text{C}]/([^{12}\text{C}] + [^{13}\text{C}])$. Anharmonic thermal vibration of natural ($X = 0.020$) and ^{13}C diamond ($X = 0.985$) was clarified by applying the Gram–Charlier series expansion to the temperature factors. The anharmonicity of natural diamond was larger than that of ^{13}C diamond. The isotope effect on the localized electron density has also been elucidated by application of the κ refinement. ^{13}C diamond has a larger κ parameter, 0.993(1), than natural diamond, 0.931(7), which proves that the valence electron of natural diamond is more widely distributed than that of ^{13}C diamond.

1. Introduction

Thermal conductivity of diamond ($Fd\bar{3}m, Z = 8$) has been proved to be sensitive to the ^{13}C isotope concentration by Anthony *et al.* (1990), Wei, Kuo, Thomas, Anthony & Banholzer (1991) and Onn, Witek, Qiu, Anthony & Banholzer (1992). An enormous extension of the conductivity of purification of ^{12}C has received much attention. In association with the above thermal property, isotope dependence of the lattice dynamical property of diamond has also attracted interest by studies of the Raman spectra of ^{13}C -doped diamond (Chrenko, 1988; Hass, Tamor, Anthony & Banholzer, 1991), optical absorption and luminescence measurements (Collins, Lawson, Davies & Kanda, 1990), and Brillouin scattering measurement of elastic constant (Ramdas, Rodrigues, Grimsditch, Anthony & Banholzer, 1993).

The isotope influence on the cell volume is directly related to the zero-point motion and anharmonicity of the

interatomic force. The lattice constant of mixed-crystal $^{13}\text{C}_x^{12}\text{C}_{1-x}$ has been examined by Holloway, Hass & Tamor (1991). The difference in the unit-cell volume of monoatomic crystals having various isotope ratios was discussed from a thermodynamical aspect (London, 1958).

We previously re-examined the isotope effect on the lattice constant of the diamond mixed-crystal $^{13}\text{C}_x^{12}\text{C}_{(1-x)}$ by single-crystal X-ray diffractometry using synchrotron radiation (Yamanaka, Morimoto & Kanda, 1994). The diamond cell volume does not linearly decrease with increasing isotope content of ^{13}C . This would be related to the difference in the valence electron density of the mixed crystals.

Charge density and Debye–Waller factors of natural diamond based on X-ray powder diffraction data have been investigated by applying the Hartree–Fock calculation (McConnel & Sanger, 1970), generalized X-ray scattering factor (Stewart, 1973) and deformation-density model of multipole terms of the exponential form (Price & Maslen, 1978). Several other methods for improving the representation of the charge density have been proposed by Dawson (1967), Hirshfeld (1971) and Denteneer & van Haeringen (1985) by the pseudopotential-density-functional method.

Many papers have also been reported discussing Reninger's effect or the 'forbidden' reflections of diamond which result from the nonsphericity of electron density (Tischler & Batterman, 1984; Kotani & Yamanaka, 1991). However, neither theoretical nor experimental investigation has ever been made on the isotope influence on charge density. In this experiment, the influence of the isotope ratio on the localized charge density has also been clarified by introducing the κ -refinement (Coppens, Guru Row, Stevens, Becker & Yang, 1979; van der Wal & Stewart, 1984).

Besides the difference in the localized charge density with isotope ratio, we elucidated the anharmonic potential of atomic thermal vibration of natural and ^{13}C diamond using the Gram–Charlier expansion (Johnson & Levy, 1974) for the purpose of understanding the difference in their thermal conductivity.

2. Experimental

2.1. Sample preparation

Single crystals of diamond with various isotope ratios between ^{13}C and ^{12}C have been synthesized using high-pressure apparatus (Kanda, Ohsawa, Fukunaga & Sunagawa, 1989). The isotope ratios of the grown diamond specimens as well as natural diamond were determined by a secondary ion mass spectrometer (Hitachi-IMA2A SIMS). The isotope content was measured using the O^{2+} primary ion beam on the crystal surface of $100\ \mu\text{m}$ across for a sputtering time of 1 h. The isotope ratio represents the mean value of more than five observed data. The observed ratios $[^{13}\text{C}]/([^{12}\text{C}] + [^{13}\text{C}])$ in the natural and four synthesized diamonds were proved to be 2.0 ± 0.8 , 18.3 ± 1.1 , 48.1 ± 1.0 , 67.3 ± 1.1 and $98.5 \pm 0.4\ \text{wt}\%$. Crystals of *ca.* $20\ \mu\text{m}$ in radius were selected for the single-crystal diffraction studies.

2.2. Diffraction study using synchrotron radiation

In comparison with the conventional laboratory X-ray source, the positron synchrotron radiation at the Photon Factory provides an extremely collimated X-ray beam of 1 (vertical) and 4.5 mrad (horizontal), which was emitted from a normal bending magnet with maximum energies 2.5 GeV and 300 mA. The wavelength finely monochromated by the Si 111 crystal plate was $\lambda = 0.697148 \pm 2.8 \times 10^{-5}\ \text{\AA}$, which was confirmed by the diffraction of a silicon crystal with the lattice constant $a = 5.430940 \pm 3.0 \times 10^{-5}\ \text{\AA}$. The monochromator provides us with a high energy-resolution of $\Delta\lambda/\lambda = 4 \times 10^{-5}$ and produces a small broadening of radiation. The present study was made by a vertical four-circle diffractometer installed in BL-10A at the Photon Factory. The specification about the diffractometer was detailed in the Photon Factory Activity Report (Tagai *et al.*, 1983).

The lattice constants of five samples were measured by profile fitting of 25 reflections for each specimen. The Bragg angle was measured by the mode of Bond method (Bond, 1960), $\theta = \pm 90^\circ + (\theta_1 + \theta_2)/2$. The profile fitting was applied to the step-counted intensities by the pseudo-Voigt function and provided an accurate intensity, together with peak position, full width at half maximum, FWHM (Γ), and Gaussian fraction (η parameter)

$$P(2\theta_i) = c[\eta Gi(2\theta_i) + (1 - \eta)Li(2\theta_i)]. \quad (1)$$

where $Li(2\theta_i)$ and $Gi(2\theta_i)$ are Lorentzian and Gaussian functions, respectively. The peak position of each reflection fell into precision within 9 s. FWHM's of most of the reflections were *ca.* 0.05° in 2θ (equivalent to 180 s). Temperature in the hutch of the PF experimental station was finely controlled at $299 \pm 0.5\ \text{K}$, for fear that the thermal expansion should affect the lattice constant,

because of an extremely small change in the lattice constant with the isotope ratio. We performed the lattice constant measurement with precision of the order $10^{-5}\ \text{\AA}$. A more detailed presentation on the diffractometry and calculation is described in our previous paper (Yamanaka, Morimoto & Kanda, 1994).

The diffraction intensities were measured for two end-components of the isotope solid solution, natural (2.0 wt%) and ^{13}C (98.5 wt%) diamond. After the positioning of 2θ , ω , φ and χ axes, based on the orientation matrix determined in advance, each reflection was measured using the ω - 2θ step scanning mode which accurately scans the peak top. In consideration of the step width to the FWHM larger than 0.05° in 2θ , the mode was conducted with an increment of 0.01° in 2θ and a scanning speed of 1 s per step. Most of the diffraction peak profiles are represented by more than 50 steps. Diffraction intensities of reflections in a minimum asymmetric reciprocal space were observed up to $\sin\theta/\lambda = 1.189\ \text{\AA}^{-1}$ ($hkl = 822$ and 660). Normalization of the incident beam intensity was made by measuring the intensities of two reference reflections every 5 observed data in order to conquer the current decay of the synchrotron radiation with time. The observed integrated intensities were corrected for Lorentz and polarization factors. A full-matrix least-squares refinement was executed using the diffraction intensities of 23 crystallographically independent reflections. An absorption correction for the spherical specimen was applied for the integrated intensity. However, it was extremely small ($\mu r = 2.75 \times 10^{-3}$), because of a very small sample ($r = 20\ \mu\text{m}$) and short wavelength.

2.3. κ -parameter and anharmonic thermal vibration

Firstly, the conventional least-squares refinement included only an anisotropic temperature factor β_{ij} and isotropic extinction parameter G_{ex} . The isotropic extinction parameter was refined on the basis of a type I model (Becker & Coppens, 1974). The present investigation requires the precise refinement of the static electron density of C atoms and their thermal motion in diamond structure. In the least-squares calculation, parameters estimating anisotropic valence electron distribution have strong correlations with parameters describing the thermal atomic motion. Therefore, in the first stage the electron distribution adopted was a monopole model in disregard of the anharmonicity of the thermal motion. The charge density of the valence electrons was elucidated by κ refinement (Coppens, Guru Row, Stevens, Becker & Yang, 1979; van der Wal & Stewart, 1984) on the basis of the structure factor $F(hkl)$. The following atomic scattering factor (f), which was modified from a Hartree-Fock approximation for the isolated atom model, was accounted for the refinement.

In the present study, the deformation of the valence electron distribution is only considered. Then the atomic

scattering factor is

$$f(S/2) = fC^{4+}(S/2) + [fC^0(S/2\kappa) - fC^{4+}(S/2\kappa)] + f' + if'' \quad (2)$$

where $S = 2 \sin \theta / \lambda$, κ is a parameter of the radial distribution of electrons in the wavefunction, fC^{4+} can be assigned to the atomic scattering factor of 1s electrons of the core and fC^0 represents the atomic scattering factor of the total 1s, 2s and 2p electrons of non-ionic atoms. f' and f'' are anomalous dispersion terms. An fC^0 table of $\sin \theta / \lambda$ at an interval of 0.01 \AA^{-1} is taken by the interpolation of data obtained from *International Tables for X-ray Crystallography* (1974, Vol. IV) and fC^{4+} are from Fukamachi (1971).

In the second stage deviations from the harmonic thermal motion of C atoms was considered for temperature factors $T(h)$. We applied the anharmonic thermal motion which is based on the following three-dimensional Gram-Charlier expansion (Johnson & Levy, 1974) of the trivariate Gaussian probability density function

$$T(h) = \exp(-\beta_{pq}h_p h_q) [1 + \{(2\pi i)^3 / 3!\} c_{pqr} h_p h_q h_r + \{(2\pi i)^4 / 4!\} d_{pqrs} h_p h_q h_r h_s + \{(2\pi i)^5 / 5!\} e_{pqrst} h_p h_q h_r h_s h_t + \dots], \quad (3)$$

where β_{pq} denotes the anisotropic temperature factor and h indicates the reflection indices. The anharmonic thermal parameters up to fourth-rank coefficients were reliable in the least-squares refinement, because the parameters over the correlation of the 5th rank is too high to offer any meaningful values. The temperature parameters higher than 5th rank in (3) were truncated in the present refinement. The only four thermal parameters of $\beta_{11} (= \beta_{22} = \beta_{33})$, c_{123} , $d_{1111} (= d_{2222} = d_{3333})$ and $d_{1122} (= d_{1133} = d_{2233})$ are independent variables for the $4/3m$ site symmetry of C atoms in the diamond structure.

The full-matrix least-squares refinement, including the anharmonic thermal parameters and κ parameter, has been carried out using the program *RADY* (Sasaki & Tsukimura, 1987).

3. Result

3.1. Lattice constant

The precise measurement of the diffraction angle and profile analysis revealed the difference in the lattice constant with nuclear mass. The lattice constants of five samples of diamond mixed crystals between ^{12}C and ^{13}C vary with the isotope ratio, as shown in Table 1. Their cell volumes and interatomic C—C distances are also presented in Table 1. The variation of the lattice constant can be expressed by the following quadratic equation

(Yamanaka, Morimoto & Kanda, 1994)

$$a(\text{\AA}) = 3.56712(5) - [9.01(5) \times 10^{-4} X] + [3.65(4) \times 10^{-4} X^2], \quad (4)$$

where X is a fraction of $X = {}^{13}\text{C} / ({}^{12}\text{C} + {}^{13}\text{C})$. Holloway, Hass & Tamor (1991), however, reported a linear relation of the lattice constant to the isotope ratio. The difference of the lattice constant between natural diamond and ^{13}C diamond is found to be extremely small, $\Delta a = a_{0.02} - a_{0.99} = -5.4 \times 10^{-4} \text{ \AA}$, with the fractional difference $\Delta a / a_{0.02} = -1.51 \times 10^{-4}$.

3.2. Difference in the κ refinement

The difference in the deformation of electron cloud between ^{12}C and ^{13}C diamond has been investigated by κ refinement. The refinement starts from the least-squares calculation procedure based on the harmonic oscillation model. Since the κ parameter has a large correlation with thermal parameters, the subsequent refinement of anisotropic anharmonic thermal parameters refrains from the multipole refinement of the electron density. Following the refinements, including anisotropic thermal and extinction parameters, the reliability factor of the least-squares calculation $R = [\sum |F_o| - |F_c|] / \sum |F_o|$ was calculated as 0.0082 and 0.0098 for natural and ^{13}C diamond, respectively.

At this stage κ refinement was carried out by introducing the atomic scattering factor, as expressed by equation (2). The κ parameter refined in full-matrix least-squares calculations for both samples indicates that ^{13}C diamond has a larger κ value [$\kappa = 0.993(1)$] than natural diamond [$\kappa = 0.931(7)$]. These parameters infer that the valence electron of natural diamond is more widely distributed than that of ^{13}C diamond. This is probably related to the difference in zero-point motion of the atoms in both diamonds.

3.3. Isotope effect on the anharmonic thermal vibration

Fourier synthesis in the (110) plane based on the harmonic thermal vibration for natural and ^{13}C diamond exhibits a considerably large bonding electron density between two atoms, which agrees well with the theoretical total-valence electronic charge-density by self-consistent pseudopotential calculation (Denteneer & van Haeringen, 1985; Chelikowsky & Cohen, 1974). The bonding electron-density feature reveals few differences between natural and ^{13}C diamond. The difference-Fourier map shown in Fig. 1 exhibits nonspherical residual electron density around the atoms, which is related to the anharmonic thermal vibration of atoms. The refinement, including anharmonic thermal parameters based on (3), was succeeded to the κ refinement. The converged parameters are presented in Table 2. The final reliability parameters become $R = 0.0078$ and $wR = 0.0081$ for natural diamond and $R = 0.0088$ and

Table 1. Lattice constant of $^{13}\text{C}_x^{12}\text{C}_{(1-x)}$ diamond

X	a (Å)	V (Å ³)	V/V ₀	d (Å)
0.02 (1)	3.56712 (5)	45.3892 (1)	1.00000	1.54460 (2)
0.18 (1)	3.56693 (8)	45.3820 (2)	0.99981	1.54452 (3)
0.48 (1)	3.56679 (9)	45.3767 (3)	0.99966	1.54446 (4)
0.67 (1)	3.56667 (9)	45.3721 (3)	0.99958	1.54440 (4)
0.985 (4)	3.56658 (7)	45.3686 (2)	0.99954	1.54436 (3)

X indicates the isotope ratio $^{13}\text{C}/(^{12}\text{C} + ^{13}\text{C})$. V/V_0 is the volume ratio, based on the cell volume of natural sample. d (Å) denotes the C—C bond distance.

$wR = 0.0140$ for ^{13}C diamond.

The temperature $T(h)$ is expressed by the Fourier transform of the probability density function $P(u)$. The one-particle potential (OPP) $V(u)$ derived from thermal parameters has been proposed from statistical thermodynamics by Willis (1969) and Mair & Wilkins (1976). Kontio & Stevens (1982) proposed the OPP equation on the basis of the Gram-Charlier expansion of thermal parameters. In the present study anharmonicity of diamond structure at room temperature shows a small deviation from the harmonic potential. Then the following approximation proposed by Kontio & Stevens (1982) was applied to $\exp[-V(u)/k_B T]$ using $e^x \approx 1 + x$, when x is small. The anharmonic potential is represented by the following form

$$\begin{aligned} \exp[-V(u)/k_B T] = & \exp(i^2 \alpha / 2k_B T \cdot \mathbf{u}^2) [1 + i^3 \beta / k_B T \cdot u_1 u_2 u_3 + i^4 \gamma / k_B T \cdot \mathbf{u}^4 \\ & + i^4 \delta / k_B T (u_1^4 + u_2^4 + u_3^4 - 3/5 \cdot \mathbf{u}^4)], \end{aligned} \quad (5)$$

where $\mathbf{u}^4 = (u_1^2 + u_2^2 + u_3^2)^2$.

Temperature parameters represented by the Gram-Charlier expansion are equivalent to the equation introduced from (5).

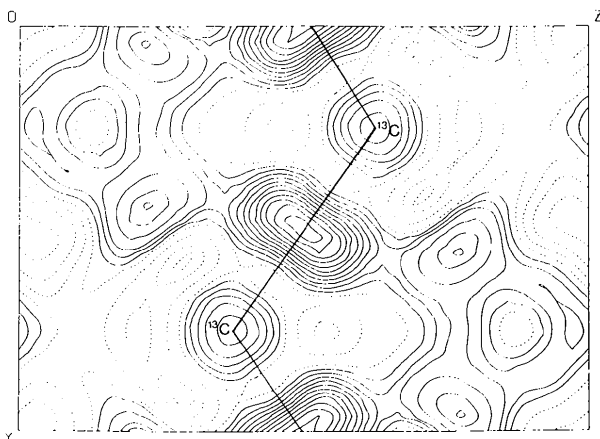


Fig. 1. Difference-Fourier map of ^{13}C diamond in the (110) plane after the refinement of the harmonic thermal parameter and κ refinement. The unit contour is $0.02 \text{ e } \text{Å}^{-3}$. The map reveals the bonding electron and residual electron density around the C atoms, which is related to the anharmonic thermal vibration of atoms.

$$\begin{aligned} T(h) = & \exp[-k_B T / \alpha (2\pi/a)^2 \cdot \mathbf{h}^2] \{1 - k_B T (15\gamma/\alpha^2 - \beta^2/2\alpha^3) \\ & + (k_B T)^2 (2\pi/a)^2 (10\gamma/\alpha^3 - \beta^2/2\alpha^4) h^2 \\ & + i(k_B T)^2 (2\pi/a)^3 \beta/\alpha^3 h_1 h_2 h_3 \\ & - (k_B T)^3 (2\pi/a)^4 (\gamma/\alpha^4) \cdot \mathbf{h}^4 \\ & - 2/5 (k_B T)^3 (2\pi/a)^4 (\delta/\alpha^4) [h_1^4 + h_2^4 + h_3^4 \\ & - 3(h_1^2 h_2^2 + h_1^2 h_3^2 + h_2^2 h_3^2)] \\ & + (k_B T)^3 (2\pi/a)^4 (\beta^2/2\alpha^5) (h_1^2 h_2^2 + h_1^2 h_3^2 + h_2^2 h_3^2)\}, \end{aligned} \quad (6)$$

where a is the lattice constant, and α , β , γ and δ are the potential parameters in (5).

Thermal parameters obtained from the least-squares refinement in consideration of the site symmetry of $43m$ are expressed using the potential parameters (Kontio & Stevens, 1982)

$$\begin{aligned} 2\pi^2 \beta_{11} &= (2\pi/a)^2 \{k_B T / 2\alpha - (k_B T)^2 \\ & \times [10\gamma/\alpha^3 - \beta^2/\alpha^4]\} \\ (4\pi^3/3) c_{123} &= -i(k_B/T)^2 (2\pi/a)^3 \beta/\alpha^3 \\ (2\pi^4/3) d_{1111} &= -(k_B/T)^3 (2\pi/a)^4 (\gamma/4 + \frac{2}{3} \delta/\alpha^4) \\ (2\pi^4/3) d_{1122} &= (k_B/T)^3 (2\pi/a)^4 \\ & \times (2\gamma/\alpha^4 - \frac{6}{5} \delta/\alpha^4 - \beta^2/2\alpha^5). \end{aligned} \quad (7)$$

The difference-Fourier map in the (110) plane of ^{13}C diamond after anharmonic refinement is presented in Fig. 2. The refinement resulted in a slightly larger anisotropic anharmonic thermal vibration, C_{123} , of natural diamond than that of ^{13}C .

The potential parameters of OPP, α , β , γ and δ calculated from the thermal parameters of β_{11} , c_{123} , d_{1111} and d_{1122} , are presented in Table 2. The potential curves $V(u)$ of ^{13}C in the direction parallel to [111], [110] and [100] are shown in Fig. 3. The anharmonic potential curves along the [111] direction concerning natural and ^{13}C diamond are shown in Fig. 4. The anharmonicity is more noticeable in the [111] direction, compared with [110] and [100] in both samples.

4. Discussion

Lattice dynamic studies (Chrenko, 1988; Hass, Tamor, Anthony & Banholzer, 1992) reveal that lattice vibrations differ between ^{12}C and ^{13}C diamond and suggest that phonon coupling with electronic state may induce the difference. The Raman peak-shift previously observed as a function of isotope concentration in diamonds confirms that the frequency ratio $\omega(X)^2/\omega(0)^2$ in the whole solid solution range was not simply varied in a linear relation with the isotope content (X). The nonlinear change in frequency is coincident

Table 2. Analysis of anharmonic thermal parameters

	Natural diamond	^{13}C diamond
^{13}C concentration (%)	2.0 (8)	98.5 (4)
Lattice constant (\AA)	3.56712 (5)	3.56658 (7)
Volume (\AA^3)	4.3892 (1)	45.3686 (2)
$R(F)$	0.0078	0.0088
$wR(F)$	0.0081	0.0140
No. of data	23	23
B_{iso} (\AA^2)	0.090 (2)	0.146 (4)
\bar{u}^2 (\AA^2)	0.036	0.043
κ parameter	0.931 (7)	0.993 (1)
$G_{\text{iso}} \times 10^{-4}$	0.273 (19)	0.210 (11)
$\beta_{11} \times 10^4$	18 (4)	29 (7)
$c_{123} \times 10^6$	-6 (4)	-4 (4)
$d_{1111} \times 10^8$	-0.7 (7)	-0.8 (7)
$d_{1122} \times 10^8$	13 (10)	21 (13)
$\alpha \times 10^{20}$ (J \AA^{-3})	18.62	11.36
$\beta \times 10^{20}$ (J \AA^{-3})	10.21	1.668
$\gamma \times 10^{20}$ (J \AA^{-3})	-1.301	-0.3953
$\delta \times 10^{20}$ (J \AA^{-3})	-3.467	1.0222

with the variation of the lattice constant previously reported (Yamanaka, Morimoto & Kanda, 1994).

The diamond interatomic distance d is calculated from the observed lattice constant $1.54460 \pm 2.0 \times 10^{-5}$ \AA for natural diamond and $1.54436 \pm 3.0 \times 10^{-5}$ \AA for ^{13}C diamond. The difference 2.4×10^{-4} \AA between the two samples is induced from both atomic thermal vibration and valence-electron distribution related to the nuclear weight. It has been clarified that the localization of the valence charge density would be more intensified in ^{13}C diamond compared with natural diamond. The experimental results concerning the interatomic distance of ^{12}C - ^{12}C and ^{13}C - ^{13}C have been explained by the electron-phonon coupling effects and structural disorder. As shown in Fig. 5, the unit-cell volume difference between natural and ^{13}C diamond is on the line with those of the monatomic crystals with various isotope ratios. The isotopic effects on unit-cell volumes is attributed to the anharmonic atomic vibration due to

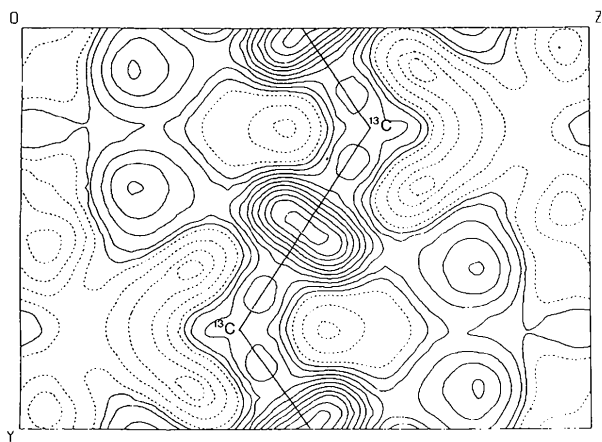


Fig. 2. Difference-Fourier map of ^{13}C diamond in the (110) plane after the refinement of the anharmonic thermal vibration. The contour interval is as in Fig. 1.

the different isotope mass. It has been discussed from a thermodynamical aspect that the fractional mass ratios $\Delta M/M$ in crystals containing different isotopes produce an effect on their fractional volume ratio $\Delta V/V$ (London, 1958; Buschert, Merlini, Pace, Rodriguez & Grimsditch, 1988).

In order to comprehend the difference in the lattice constant due to the isotope ratio, the anisotropic anharmonic thermal potential of atoms has been discussed on ^{12}C and ^{13}C isotopes in this study. The observed anharmonic parameters of d_{1111} and d_{1122} are indeed small, but the term of c_{123} indicating the

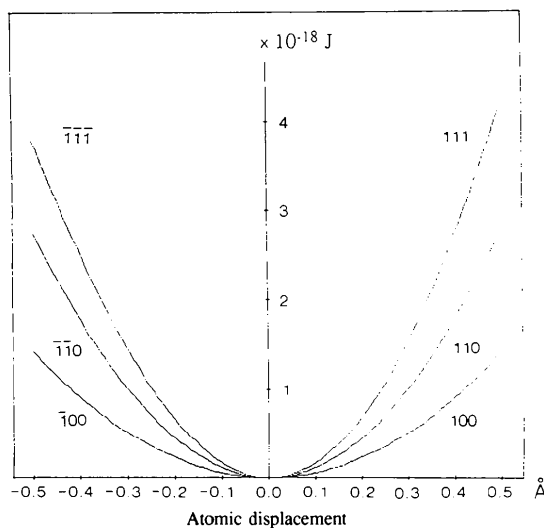


Fig. 3. Anharmonic potential of ^{13}C diamond in the direction parallel to [100], [110] and [111]. Anisotropic anharmonicity in the atomic vibration is observed only in the direction of [111].

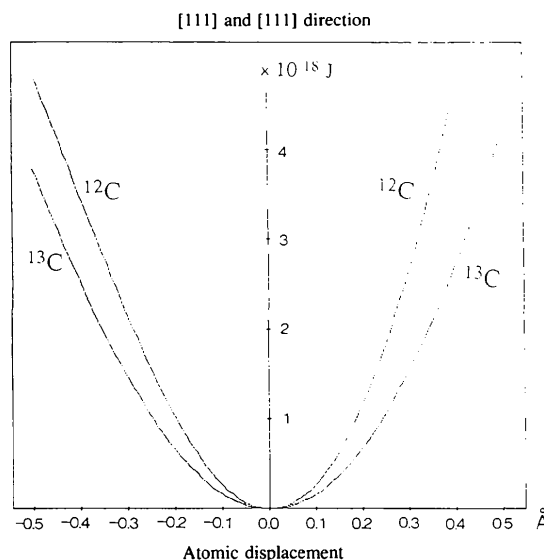


Fig. 4. Anharmonic potential curve in the [111] and [111] directions of natural and ^{13}C diamond.

anisotropic anharmonic thermal vibration is still large enough to be considered. Both the difference-Fourier map of the residual electron density shown in Fig. 2 and the anharmonic potential curve in Fig. 4 indicate that the anisotropic anharmonicity is dominant in the (111) direction.

One of the authors previously investigated the anharmonic thermal motion of atoms in MgAl_2O_4 at various temperatures or in ZnX ($X = \text{S, Se, Te}$) with different bonding character. The refinements of MgAl_2O_4 spinel at elevated temperatures up to 1933 K (Yamanaka, Takeuchi & Tokonami, 1984) and ZnX ($X = \text{S, Se}$ or Te) zinc blende structures (Yamanaka, Takeuchi & Tokonami, 1985) both reveal an extreme anharmonicity of cations in the $\bar{4}3m$ site, Mg ions in the former and Zn ions in the latter. These materials are composed of more ionic bonding character compared with diamond. The covalency in diamond was expressed by the noticeable bonding electron density between atoms, as shown in Fig. 2. This may prove from the present study that the valence electron in ^{13}C diamond is more localized than in natural diamond.

The thermal atomic motion in diamond is restricted at room temperature, because of the extremely high Debye temperature (2340 K) and large stiffness tensors of elastic constants, $c_{11} = 1079 \pm 5$, $c_{12} = 124 \pm 5$ and $c_{44} = 578 \pm 2$ GPa (McSkimin & Andreatch, 1972). Consequently, diamond has a remarkably small thermal expansion coefficient of $0.81 \times 10^6 \text{ K}^{-1}$ around ambient temperature (Slack & Bartram, 1975). Thus, the anharmonicity of atomic thermal motion of diamond is very small at room temperature. The anharmonic potential of diamond will be more intensively shown by an *in situ* X-ray diffraction study at high temperature.

The authors are indebted to Dr C. Uyeda of Department of Earth and Space Science, Osaka Uni-

versity, for the measurement of isotope ratio by SIMS. They also express their great thanks to Dr H. Kanda of National Research Institute in Inorganic Material for kindly providing the sample of diamond.

References

- Anthony, T. R., Banholzer, W. F., Fleicher, J. F., Wei, L., Kuo, P. K., Thomas, R. L. & Priour, R. W. (1990). *Phys. Rev. B*, **42**, 1104–1111.
- Becker, P. J. & Coppens, P. (1974). *Acta Cryst.* **A30**, 129–147.
- Bolz, L. H. & Maner, F. A. (1962). *Adv. X-ray Anal.* **6**, 242–251.
- Bond, W. L. (1960). *Acta Cryst.* **13**, 330–336.
- Buschert, R. C., Merlini, A. E., Pace, S., Rodriguez, S. & Grimsditch, M. H. (1988). *Phys. Rev. B*, **38**, 5219–5221.
- Chelikowsky, J. R. & Cohen, M. L. (1974). *Phys. Rev. Lett.* **33**, 1339–1342.
- Chrenko, R. M. (1988). *J. Appl. Phys.* **63**, 5873–5875.
- Collins, A. T., Lawson, S. C., Davies, G. & Kanda, H. (1990). *Mater. Sci. Forum*, **65/66**, 199–204.
- Coppens, P., Guru Row, T. N., Stevens, E. D., Becker, P. J. & Yang, Y. W. (1979). *Acta Cryst.* **A35**, 63–72.
- Covington, E. J. & Montgomery, D. J. (1957). *J. Chem. Phys.* **27**, 1030–1032.
- Dawson, B. (1967). *Proc. R. Soc. A*, **298**, 264–288.
- Denteneer, P. J. H. & van Haeringen, W. (1985). *J. Phys. C*, **18**, 4127–4142.
- Fukamachi, T. (1971). Technical Report B12. Institute of Solid State Physics, University of Tokyo.
- Hass, K. C., Tamor, M. A., Anthony, T. R. & Banholzer, W. F. (1991). *Phys. Rev. B*, **44**, 12046–12049.
- Hass, K. C., Tamor, M. A., Anthony, T. R. & Banholzer, W. F. (1992). *Phys. Rev. B*, **45**, 7171–7182.
- Hirshfeld, F. L. (1971). *Acta Cryst.* **B27**, 769–781.
- Holloway, H., Hass, K. C. & Tamor, M. A. (1991). *Phys. Rev. B*, **44**, 7123–7126.
- Johnson, C. K. & Levy, H. A. (1974). *International Tables for X-ray Crystallography*, Vol. IV, pp. 311–336, Birmingham: Kynoch Press. (Present distributor Kluwer Academic Publishers, Dordrecht.)
- Kanda, H., Ohsawa, T., Fukunaga, O. & Sunagawa, I. (1989). *J. Cryst. Growth*, **94**, 115–124.
- Kogan, V. S. & Bulatov, A. S. (1962). *Zh. Eksp. Teor. Fiz.* **42**, 1499. Translation: *Soviet Physics-JETS* **15**, 1041–1043.
- Kontio, A. & Stevens, E. D. (1982). *Acta Cryst.* **A38**, 623–629.
- Kotani, T. & Yamanaka, T. (1991). *Phys. Rev. B*, **44**, 6131–6136.
- London, H. (1958). *Z. Phys. Chem. Neue Folge*, **16**, 302–309.
- Mair, S. L. & Wilkins, S. W. (1976). *J. Phys. C*, **9**, 1145–1158.
- McConnel, J. F. & Sanger, P. L. (1970). *Acta Cryst.* **A26**, 83–93.
- McSkimin, H. J. & Andreatch, P. (1972). *J. Appl. Phys.* **43**, 2944–2948.
- Onn, D. G., Witek, A., Qiu, Y. Z., Anthony, T. R. & Banholzer, W. F. (1992). *Phys. Rev. Lett.* **68**, 2806–2809.
- Price, P. F. & Maslen, E. N. (1978). *Acta Cryst.* **A34**, 173–183.
- Ramdas, A. K., Rodriguez, S., Grimsditch, M., Anthony, T. R. & Banholzer, W. F. (1993). *Phys. Rev. Lett.* **71**, 189–192.

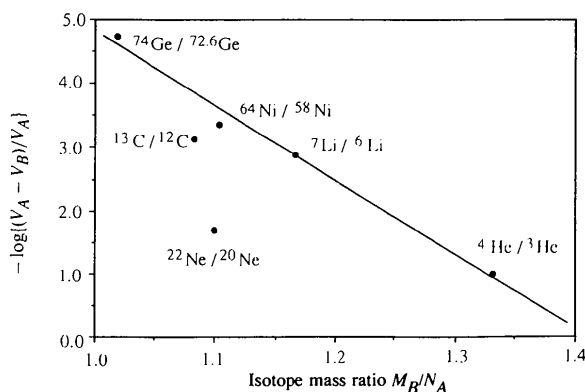


Fig. 5. Cell-volume difference of monoatomic crystals with different isotopes. The volume differences are plotted as a function of the mass ratio of monoatomic crystals. ^3He and ^4He (Wilkins, 1967), ^{20}Ne and ^{22}Ne (Bolz & Maner, 1962), ^{72}Ge and ^{74}Ge (Buschert, Merlini, Pace, Rodriguez & Grimsditch, 1988), ^6Li and ^7Li (Covington & Montgomery, 1957), and ^{58}Ni and ^{64}Ni (Kogan & Bulatov, 1962).

- Sasaki, S. & Tsukimura, K. (1987). *J. Phys. Soc. Jpn*, **56**, 437–440.
- Slack, G. A. & Bartram, S. F. (1975). *J. Appl. Phys.* **46**, 89–98.
- Stewart, R. F. (1973). *J. Chem. Phys.* **58**, 4430–4438.
- Tagai, T., Tokonami, M., Sakamaki, T., Sato, Y., Ohsumi, K., Nakazawa, H., Abe, T., Hirai, T., Ohmasa, M., Sueno, S., Haga, N., Kudoh, Y., Nishi, F., Tsukimura, K., Kanazawa, Y., Yamada, N., Saito, S., Kakefuda, K., Watanabe, M., Nukui, A., Kawada, I., Okamura, F., Nakai, I., Sugiyama, K., Nakanishi, K., Ogata, K., Sasaki, S. & Takeuchi, Y. (1983). Photon Factor Activity Report. VI-19.
- Tischler, J. Z. & Batterman, B. W. (1984). *Phys. Rev. B*, **30**, 7060–7066.
- Wal, R. J. van der & Stewart, R. F. (1984). *Acta Cryst.* **A40**, 587–593.
- Wei, L., Kuo, P. K., Thomas, R. L., Anthony, T. R. & Banholzer, W. F. (1991). *New Diamond Science and Technology*, pp. 875–880. MRS Int. Conf. Proc.
- Wilks, J. (1967). *The Properties of Liquid and Solid Helium*, pp. 678–679. Oxford: Clarendon Press.
- Willis, B. T. M. (1969). *Acta Cryst.* **A25**, 277–300.
- Yamanaka, T., Morimoto, S. & Kanda, H. (1994). *Phys. Rev. B*, **49**, 9341–9343.
- Yamanaka, T., Takeuchi, Y. & Tokonami, M. (1984). *Acta Cryst.* **B40**, 96–102.
- Yamanaka, T., Takeuchi, Y. & Tokonami, M. (1985). *Acta Cryst.* **B41**, 298–304.